Effective transport of passive particles induced by chiral-active particles in microchannel*

Yunfeng Hua(华昀峰)[1], Linli He(何林李)[2], and Linxi Zhang(章林溪)[1,†]

[1]*Department of Physics, Zhejiang University, Hangzhou* 310027, *China*
[2]*Department of Physics, Wenzhou University, Wenzhou* 325027, *China*

(Received 27 March 2017; revised manuscript received 2 May 2017; published online 20 June 2017)

Transport of passive particles induced by chiral-active particles in microchannel is investigated by using the overdamped Langevin dynamics simulation in a two-dimensional model system. Due to the chirality of active particles and special structure of microchannel, effective ratchet transport of passive particles is achieved. Effective transport of passive particles depends on the width of microchannel (d), the density (ρ), and the angular velocity (ω) of chiral-active particles. There exist optimal parameters for d and ω at which the transport efficiency for passive particles takes its maximal value. This investigation can help us understand the necessity of active motion for living systems to maintain a number of vital processes such as materials transport inside cells and the foraging dynamics of mobile organisms.

Keywords: transport, active particle, passive particle, overdamped Langevin dynamics simulation, microchannel

PACS: 07.05.Tp, 77.84.Jd, 78.40.Pg, 78.67.Qa **DOI:** 10.1088/1674-1056/26/8/080702

1. Introduction

The transport of particles confined in a narrow channel has attracted considerable attention because of its importance in many processes, from chemistry, physical and biological to complex systems.[1,2] Active particles are small scale materials capable of producing enhanced motion with fluid environments, and assumed to have an internal propulsion mechanism, which can use energy from an external source and transform them under non-equilibrium conditions into the directed motion. In the biological realm, many cells perform active Brownian motion, for example, microorganisms like bacteria, sperm cells or other eukaryotic cells employ various strategies to generate directed motion in a fluid environment.[3,4] Since active particles can transport without external drives, they can be used as a "nanorobot" for applications in the medical sciences and nanotechnology. Therefore, there has been a growing interest in understanding self-propulsion.[5,6] Actually, self-propulsion is the ability of most living organisms to move in the absence of external drives by means of an internal "engine" of their own. Compared with passive particles, active particles moving in confined structures could exhibit special behaviors, resulting for example in collective motion in complex systems,[7] accumulating of particles in the proximity of the wall, trapping of particles in microwedge,[8] spontaneous rectified transport,[5,6,9–16] width of particles based on their swimming properties,[17–22] spiral vortex formation in the circular confinement,[23] depletion of elongated particles from low-shear regions,[24] upstream swimming in microchannel with capillary flow,[25,26] net particle flux in static potentials,[27] and the other interesting transport phenomena.[28–33]

There also has been increasing interest in theoretical work on the rectification of active particles.[5,6,11,12] The rectification phenomenon of overdamped swimming bacteria was theoretically observed in a system with an array of asymmetric barriers.[5] A well known rectification theorem states that the asymmetry can only emerge if spatial symmetry breaking is accompanied by time-reversal asymmetry in the trajectories.[34] Ghosh *et al*. studied the transport of Janus particles in a compartmentalized channel and found that the rectification can be orders of magnitude stronger than that for ordinary thermal potential ratchets.[5,6] Angelani *et al*.[11] studied Brownian motions of the run-and-tumble particles in periodic potentials and found that the asymmetric potential can produce a net drift speed.[11] Potosky *et al*. found that the spatially modulated self-propelled velocity can drive the directed transport of particles.[27] Huang *et al*. found that the reaction rate of the catalytic motor reaction decreases in a crowed medium as the volume fraction of obstacles increases as a result of a reduction in the Smoluchowski diffusion-controlled reaction rate coefficient that contributes to the overall reaction rate.[35] While some ability to transport materials within a fluid environment is provided by Brownian motion and osmotic effects, in many cases these phenomena do not display the required speed or directionality, especially for passive particles. In this paper, a novel microchannel with short cantboards arrayed in the middle of the channel is built, and we numerically study the transport of passive particles in this specific microchannel,

*Project supported by the National Natural Science Foundation of China (Grant Nos. 21374102, 21674096, and 21674082).
†Corresponding author. E-mail: lxzhang@zju.edu.cn
© 2017 Chinese Physical Society and IOP Publishing Ltd

where the big passive particles are immersed in the 'sea' of chiral-active particles. Our aim is to study the effective transport of passive particles induced by chiral-active particles in the microchannel, and this investigation can provide insight into out-of-equilibrium transport of passive particles in the microchannel.

2. Model and methods

The passive and chiral active particles are mixed in a two-dimensional channel with periodic boundary conditions in the y direction (L) and hard walls in the x direction (see Fig. 1). The small red and the big blue balls denote chiral-active and passive particles, respectively, and the distance between two walls is d. Short cantboards with an inclination angle 45° are regularly arrayed in the middle of the rectangle microchannel, and the distance along y direction between two adjacent cantboards is $d_0 = 2.0\sigma$. Here σ is the diameter of chiral-active particles. The overdamped dynamics is governed by Langevin equations for the position r_i of the center of the i-th particle and the orientation θ_i of the polar axis $u_i \equiv (\cos\theta_i, \sin\theta_i)$[21,22,34,36]

$$\partial_i \mathrm{r}_i = V_i^0 \boldsymbol{u}_i + \mu \sum_{j\neq i} \boldsymbol{F}_{ij} + \sqrt{2D_0}\boldsymbol{\xi}_i^{\mathrm{T}}(t), \tag{1}$$

$$\partial_i \theta_i = \omega + \sqrt{2D_\theta}\xi_i(t), \tag{2}$$

where μ is the mobility (i.e., $\mu = 1/\gamma$, and γ is the friction coefficient)[22] and V_i^0 is the self-propulsion speed ($V_i^0 = V_0$ for chiral active particles and $V_i^0 = 0$ for the passive particles). $\xi_i(t)$ and $\xi_i^{\mathrm{T}}(t)$ are Gaussian white noise with zero mean and correlations $\langle \xi_{i\alpha}(t)\xi_{j\beta}^{\mathrm{T}}(s)\rangle = \delta_{ij}\delta_{\alpha\beta}\delta(t-s)$ (α, $\beta = x, y$) and $\langle \xi_i(t)\xi_j^{\mathrm{T}}(s)\rangle = \delta_{ij}\delta(t-s)\langle\cdots\rangle$ denotes an ensemble average over the distribution of noise and δ the Dirac delta function. D_0 and D_θ denote the translational and rotational diffusion coefficients, respectively. ω is the angular velocity, and the force F_{ij} between particles i and j is assumed to be of the linear spring form with the stiffness constant k: $F_{ij} = k(a_i + a_j - r_{ij})$ for $a_i + a_j > r_{ij}$ and $F_{ij} = 0$ otherwise.[22] There is no angular and translation velocity of passive particles. Here a_i is the radius of particle i. The diameters of chiral active and passive particles are σ and 3.0σ, respectively. The packing fraction is defined approximately as the ratio between the area occupied by chiral active particles and the total available area, i.e., $\rho = (0.25 * N_1\sigma^2 + 2.25 * N_2\sigma^2)/(L * D - 80\sigma^2)$, where N_1 and N_2 is the number of chiral-active and passive particles, respectively, and $80\sigma^2$ is the area accounted for the cantboards. Owing to the particles being confined in the x direction, the y direction average velocity is considered here. The average velocity along the y direction in the asymptotic long-time regime can be calculated by the formula

$$V_y = \langle \lim_{t\to\infty}[y(t) - y(0)]/t\rangle, \tag{3}$$

and the scale average velocity is calculated by $V = V_y/V_0$ for convenience. Here $\langle\cdots\rangle$ is averaged over all chiral-active particles (or passive particles) and all conformations. Reduced units ($\sigma = 1$ and $1/(\mu k) = 1$ are chosen to be the units of length and time) are used. In our simulations, equations of motion are integrated with the second-order Runge–Kutta method. The time step is chosen to be $\Delta t = 0.001$, and the total integration time is more than 8×10^6. The chiral-active particles perform the counterclockwise motion with $\omega > 0$, and the parameters are chosen to be $D_0 = D_\theta = 5 \times 10^{-3}$, $L = 80.0$, and $V_0 = 0.5$.[22,33]

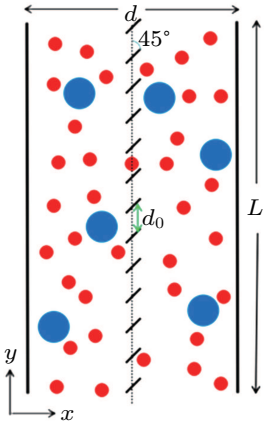


Fig. 1. (color online) A schematic diagram of chirality-power motor in a microchannel. Short cantboards are regularly arrayed in the middle of the microchannel. Periodic boundary conditions are imposed in the y direction, and the distance between two walls is d. The small red and the big blue balls denote active particles and the passive particles, respectively.

3. Results and discussion

We assume that the microchannel walls are perfectly reflecting and the particle–wall collisions are elastic.[34,35,37] In fact, for chiral-active particles, the ratchet setup demands three key ingredients which are (i) nonlinearity, (ii) asymmetry, and (iii) fluctuating input force of zero mean.[22,34] The ratchet phenomena for active particles have been investigated for a long time, and these phenomena have been understood well. However, the investigation on the ratchet transport for passive particles is rare.[22] In fact, how to transport the passive particles effectively is an interesting issue because there are wide applications such as the drug-delivery in cells and gene therapy in bioremediation.[20,22]

Figure 2 shows the scale average velocity V as a function of the distance of two hard walls d for two densities of $\rho = 0.1$ and 0.2 with $\omega = 0.05$. For chiral-active particles (denoted by the black lines), V is zero for all the values of d, and this means that no transport in a given direction occurs and only the Brownian motions are observed for chiral-active particles. Comparatively, for passive particles, the curves of the scale average velocity V for left and right passive particles are symmetrical, V is negative for left passive particles and positive for right passive ones, and the absolute value of V

is almost the same. Here left passive particles mean that the particles are located at the left microchannel, see Fig. 1. When d increases, V increases gradually from 0.048 at $d = 12$ to 0.107 at $d = 24$, followed by a decrease to $V \approx 0$ at $d = 100$ for $\rho = 0.1$. Similarly, for $\rho = 0.2$, V increases from 0.11 at $d = 12$ to 0.17 at $d = 20$, and then decreases to $V \approx 0$ at $d = 100$. Therefore, the transport of passive particles depends on the width of microchannel, and the suitable width for microchannel can induce passive particles to transport more quickly (see supplementary Video S1 and S2). In our model, microchannel is symmetry for chiral-active particles because the distance between two adjacent short cantboards ($d_0 = 2.0\sigma$) is greater than the diameter of chiral-active particles (σ), and active particles can pass through cantboards easily, therefore, the holonomic circular motions for active particles can be carried out, the scale average velocity V is close to zero and there is no transport velocity for chiral-active particles. However, for passive particles, since the distance between two adjacent short cantboards ($d_0 = 2.0\sigma$) is less than the diameter of passive particles (3σ) and they cannot pass through cantboards, the symmetry of microchannel is destroyed, especially for small d, therefore, the effective transport for passive particles is observed. In fact, the radius of circular trajectory for chiral-active particles depends mainly on ω. In a wide microchannel, such as $d = 100$, chiral-active particles can perform several holonomic circular motions, and asymmetry structures of microchannel for passive particles disappear gradually; this leads to a decrease of scale average velocity V for large d. For the passive particles, when the passive particles are immersed in the 'sea' of active particles, the interactions from active particles can break the thermodynamical equilibrium and make the passive particles move directionally.[22]

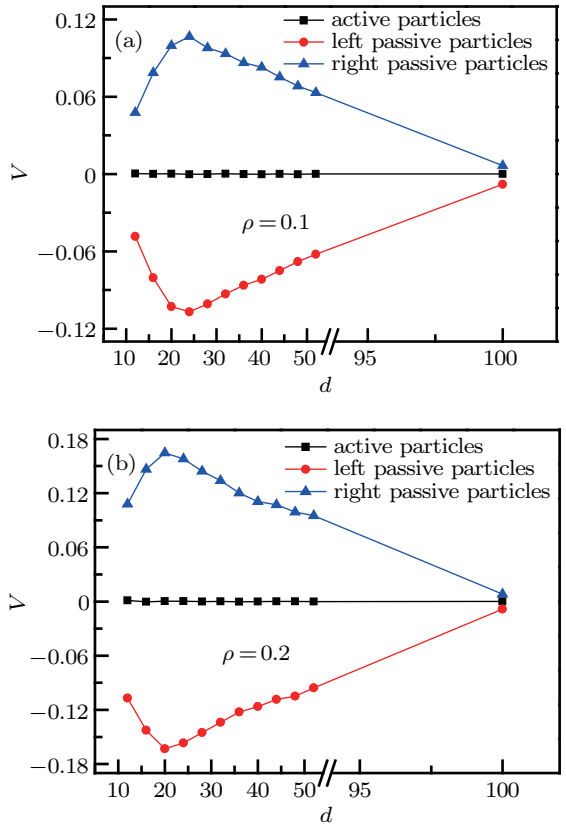


Fig. 2. (color online) Average scale velocity V of passive and active particles as a function of d for different number densities of active particles (a) $\rho = 0.1$ and (b) $\rho = 0.2$ with $\omega = 0.05$.

In Fig. 3 we present the scale average velocity V of passive and chiral-active particles as a function of the packing fraction ρ. Here, the distance between two hard walls is set to be $d = 20$ and the angular velocity is $\omega = 0.05$. For chiral-active particles, the scale average velocity V is independent of the packing fraction ρ and is close nearly to zero. However, for passive particles, it increases with the increase of ρ for small packing fractions and then keeps unchanged for $\rho > 0.7$. When the packing fraction ρ is small enough, the interactions between active particles result in an activating motion in an analogy with the thermal noise activated motion for a single stochastically driven ratchet, which dominates the directed transport, so the average velocity V increases with the packing fraction ρ increasing. However, when the packing faction increases to large enough, the interactions between chiral-active particles cause the reduction of self-propelled driving, which impedes the ratchet transport, thus the average velocity V increases more and more slowly.

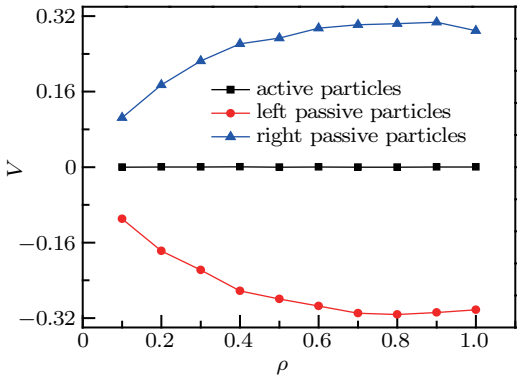


Fig. 3. (color online) Average scale velocity V of passive and active particles as a function of density ρ of active particles with $\omega = 0.05$ and $d = 20$.

In order to explain the transport mechanism of passive particles induced by active particles in the microchannel in more detail, we calculate the average impulse of passive particles suffered from the collision of chiral-active particles, which is defined as

$$I = F \times \Delta t, \tag{4}$$

where F is the total force acted by chiral-active particles and Δt is time step, i.e. $\Delta t = 0.001$. As the impulse acted by the collision of chiral-active particles depends on the position of the collision between passive and chiral-active particles, we calculate the average impulse I with different angle θ. The definition of the angle θ is shown in the inset of Fig. 4, and

the passive particles are fixed to be at $d/4$ from the left wall. In fact, the structure of microchannel affects the transport behavior of passive particles seriously, and the cantboards in the middle position of microchannel destroy the symmetry of microchannel for passive particles. Figure 4 shows the average impulse I of different angle θ for passive particle at the same relative position in the microchannel with three different cases. For the case of the width microchannel of $d = 100$ with cantboard, the passive particles suffer the left–right symmetrical impulse from the collision of active particles, and this left–right symmetrical impulse cannot cause effective transport for passive particles (see Fig. 2). For the case of the narrow microchannel of $d = 20$ without cantboard, the passive particles also suffer the uniform impulse from the collision of active particles, the passive particles always keep random motions in the narrow microchannel, and the averaged velocity is close to zero (i.e., $V \approx 0$). However, for the case of narrow microchannel ($d = 20$) with cantboard, the passive particles suffer uneven impulse form collision of active particles, and the maximum value of the impulse is located at $\theta \approx 90^\circ$ (i.e., $\pi/2$) while the minimum one is located at $\theta \approx 270^\circ$ (i.e., $3\pi/2$). This uneven impulse can cause passive particles to get an effective velocity pointed to the y direction. The more the impulse difference between $\theta \approx 90^\circ$ and 270° is, the more effective the transport of passive particles is. This uneven impulse suffered from the collision of active particles leads passive particles to transport in the microchannel directionally.

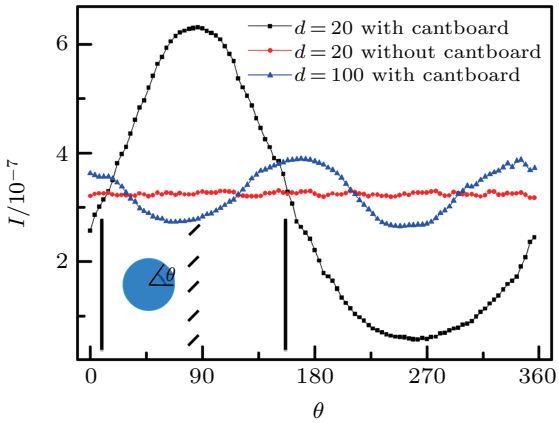


Fig. 4. (color online) Average impulses I of passive particles suffered from the collision of active particles at different positions θ with $d = 20$ and 100.

Figure 5 describes the relationship between the impulse difference value ΔI and the average velocity V as a function of (a) angular velocity ω of chiral-active particles with $d = 20$ and (b) the width d of microchannel with $\omega = 0.05$. The impulse difference ΔI is defined as $\Delta I = I_{\theta=\pi/2} - I_{\theta=\pi}$, see the inset figure in Fig. 5(a), and the trend of the impulse difference ΔI is identical with the average velocity V. If the circular trajectory chiral active particles is less than the width of microchannel, the active particles cannot perform circular motion and only slide along the walls, therefore, the active particles move directly along the negative direction of Y axis in the left area and the positive direction of Y axis in the right area, which can induce the directed transport of passive particles. As the width of microchannel d increases, the active particles show the circular motion and the transport behavior diminishes gradually for passive particles. However, when the width of microchannel d is very small, the collisions between passive particles and wall or cantboards dominate the transport, so the velocity of passive particle also decreases.

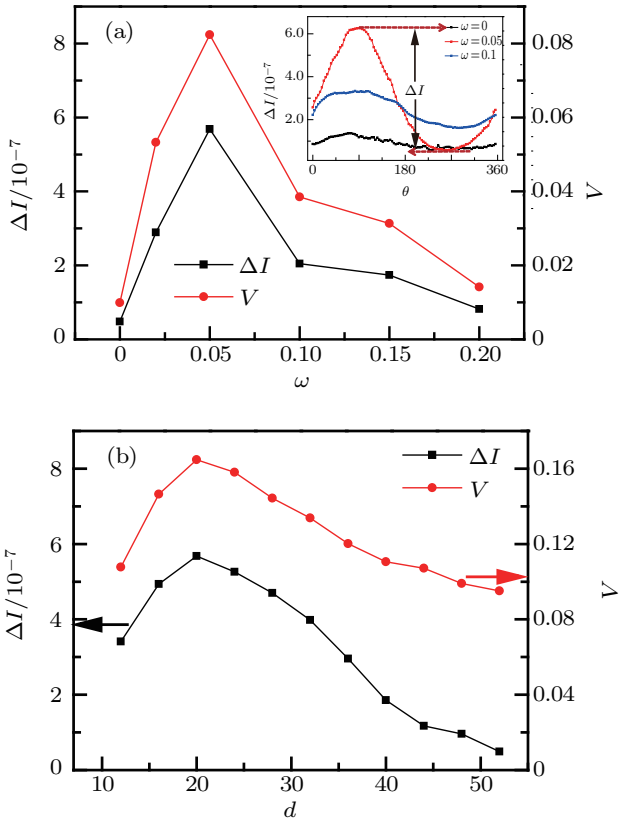


Fig. 5. (color online) The relationship between impulse difference (ΔI) and average velocity V as a function of ω with $d = 20$ (a) and d with $\omega = 0.05$ (b).

In Fig. 6, the average velocity V also depends on the angular velocity ω, and there exists an optimal value of ω at which V takes its maximal value, and the maximum value is about $V_{\max} = 0.108$ for $d = 12$ at $\omega = 0.05$, $V_{\max} = 0.158$ for $d = 24$ at $\omega = 0.05$ and $V_{\max} = 0.122$ for $d = 36$ at $\omega = 0.02$. When ω is close to 0, the circular trajectory of active particles is very large, so the active particles slide along the walls, and the passive particles move randomly in the microchannel. Therefore, the suitable angular velocity ω for active particles can cause passive particles to transport effectively in the microchannel. Of course, for the cases of large angular velocity ω, the circular trajectory of active particle decreases and the active particles only slide along the walls, therefore, the transport velocity is also small.

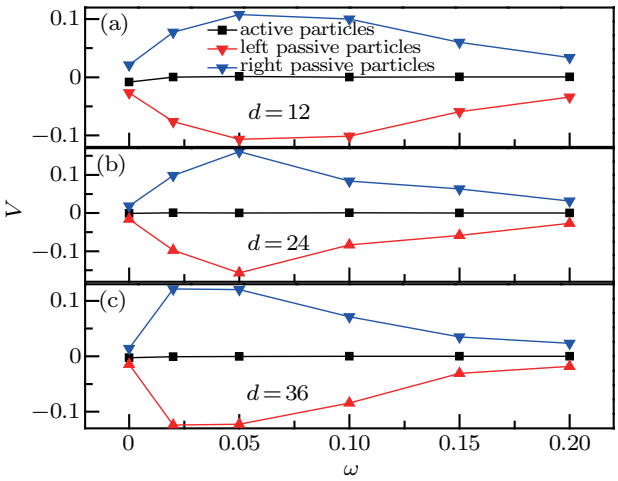


Fig. 6. (color online) Average velocity V as a function of ω with (a) $d = 12$, (b) $d = 24$, and (c) $d = 36$. Here $\rho = 0.2$.

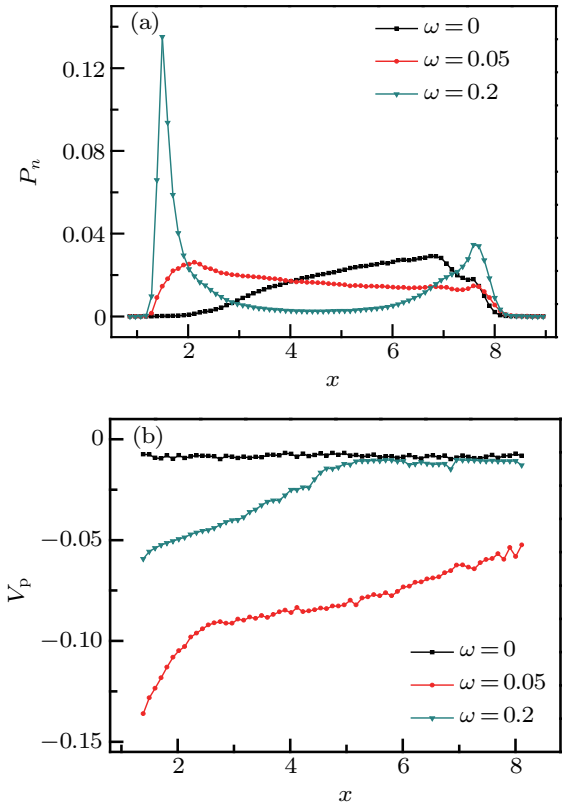


Fig. 7. (color online) Number density distribution P_n (a) and velocity distribution V_p of passive particles along x axis for different angular velocities with $d = 12$ and $\rho = 0.2$.

The position and velocity distributions of passive particles along the x direction with different angular velocities are shown in Fig. 7. As shown in Fig. 7(a), the angular velocity ω affects the spatial distributions of passive particles seriously. For the case of $\omega = 0$, the passive particles prefer to stay in the middle area, and the distribution of the passive particle moves to the left as angular velocity ω increases. As ω increases to 0.2, most of passive particles stay in the two areas near to the hard wall or cantboards. The trajectory of chiral-active particles is circular, and the radius of circular trajectory depends on the angular velocity ω. Since the radius of circular trajectory is small enough for a large angular velocity $\omega = 0.2$, the passive particles are gathered near to the wall and cantboards, especially in the wall. That is why the number density distribution for $\omega = 0.2$ has two peaks.

Meanwhile, as shown in Fig. 7(b), the velocity distribution of passive particles is almost uniform for the case of $\omega = 0$, and the velocity distribution of passive particles becomes uneven as the angular velocity ω increases, and the passive particles near to the walls have the larger velocity, especially for the case of $\omega = 0.2$. Therefore, the spatial symmetry breaking for passive particles leads to possessing a property of transport in microchannel and the effective transport of passive particles relies on the width of microchannel (d), the density (ρ), and the angular velocity (ω) of active particles.

4. Concluding remarks

Understanding the statistical properties of active matter in confined geometries is of great importance not only for basic science, but also for possible practical applications, for example in micro biomechanics, where synthetic autonomous self-propelled objects could be used as drug-delivery agents or for mechanical actuation. In this paper, we numerically studied the transport process of passive particles induced by chiral-active particles in a microchannel with short cantboards arrayed in the middle of the microchannel. As those short cantboards break out the spatial symmetry for passive particles, active particles can make passive particles move directionally. However, for active particles, as the distance between two adjacent cantboards is greater than the diameter of active particles, the spatial symmetry of microchannel for active particles remains well and there does not exist directional movements for active particles. Of course, the effective transport of passive particles depends on the width of microchannel (d), the density (ρ), and the angular velocity (ω) of active particles. There exist optimal parameters for d and ω at which the transport efficiency for passive particles takes its maximal value. This investigation can help us understand the necessity of active motion for living systems to maintain a number of vital processes such as material transport inside cells and the foraging dynamics of mobile organisms.

References

[1] Marchetti M C, Joanny J F, Ramaswamy S, *et al.* 2013 *Rev. Mod. Phys.* **85** 1143
[2] Elgeti J, Winkler R G and Gompper G 2015 *Rep. Prog. Phys.* **78** 056601
[3] Lauga E and Powers T 2009 *Rep. Prog. Phys.* **72** 096601
[4] Yang M and Ripoll M 2011 *Phys. Rev. E* **84** 061401
[5] Ghosh P K, Misko V R, Marchesoni F and Nori F 2013 *Phys. Rev. Lett.* **110** 268301

[6] Ghosh P K, Li Y, Marchesoni F and Nori F 2015 *Phys. Rev. E* **92** 012114
[7] Nepusz T and Vicsek T 2012 *Nat. Phys.* **8** 568
[8] Elgeti J and Gompper G 2013 *Europhys. Lett.* **101** 48003
[9] Cates M E 2012 *Rep. Prog. Phys.* **75** 042601
[10] Kaiser A, Peshkov A, Sokolov A, *et al.* 2014 *Phys. Rev. Lett.* **112** 158101
[11] Angelani L, Leonardo R D and Ruocco G 2009 *Phys. Rev. Lett.* **102** 048104
[12] Pototsky A, Hahn A M and Stark H 2013 *Phys. Rev. E* **87** 042124
[13] Potiguar F Q, Farias G A and Ferreira W P 2014 *Phys. Rev. E* **90** 012307
[14] Koumakis N, Maggi C and Leonardo R D 2014 *Soft Matter* **10** 5695
[15] Ai B Q, Zhu W J, He Y F and Zhong W R 2017 *J. Stat. Mech.* **17** 023501
[16] Ai B Q, He Y F and Zhong W R 2017 *Phys. Rev. E* **95** 012116
[17] Costanzo A, Elgeti J, Auth T, *et al.* 2014 *Europhys. Lett.* **107** 36003
[18] Ai B Q, He Y F and Zhong W R 2015 *Soft Matter* **11** 3852
[19] Maggi C, Lepore A, Solari J, *et al.* 2013 *Soft Matter* **9** 10885
[20] Chen J X, Guo M M and Ma J 2016 *Europhys. Lett.* **113** 38004
[21] Mijalkov M and Volpe G 2013 *Soft Matter* **9** 6376
[22] Ai B Q 2016 *Sci. Rep.* **6** 18740
[23] Wioland H, Woodhouse F G, Dunkel J, *et al.* 2013 *Phys. Rev. Lett.* **110** 268102.
[24] Rusconi R, Guasto J S and Stocker R 2014 *Nat. Phys.* **10** 212
[25] Zhang H P, Beer A, Florin E L and Swinney H L 2010 *Proc. Natl. Acad. Sci. USA* **107** 13626
[26] Hill J, Kalkanci O, Mcmurry J L and Koser H 2007 *Phys. Rev. Lett.* **98** 068101
[27] Pototsky A, Hahn A M and Stark H 2013 *Phys. Rev. E* **87** 042124
[28] Hagen B T, Kummel F, Wittkowski R, *et al.* 2014 *Nat. Commun.* **5** 4829
[29] Ai B Q and Wu J C 2014 *J. Chem. Phys.* **140** 094103
[30] Wu J C and Ai B Q 2016 *Sci. Rep.* **6** 24001
[31] Chen J X, Chen Y G and Ma Y Q 2016 *Soft Matter* **12** 1876
[32] Chen J X, Zhu J X, Ma Y Q and Cao J S 2014 *Europhys. Lett.* **106** 18003
[33] Wu J C, Zhou J N and Ai B Q 2016 *Physica A* **462** 864
[34] Volpe G, Gigan S and Volpe G 2014 *Am. J. Phys.* **82** 659
[35] Huang M J, Schofield J and Kapral R 2017 *J. Phys. A: Math. Theor.* **50** 074001
[36] Prost J, Chauwin J F, Peliti L and Ajdari A 1994 *Phys. Rev. Lett.* **72** 2652
[37] Zhang H P, Beer A, Florin E L and Swinney H L 2010 *Proc. Natl. Acad. Sci. USA* **107** 13626